10.24425/acs.2023.148885

Archives of Control Sciences
Volume 33(LXIX), 2023
No. 4, *pages 861–884*

Analysis of multiple-area renewable integrated hydro-thermal system considering artificial rabbit optimized PI (FOPD) cascade controller and redox flow battery

Arindita SAHA, Tirumalasetty CHIRANJEEVI, Ramesh DEVARAPALLI, Naladi Ram BABU, Puja DASH and Fausto Pedro GARCÍA MÁRQUEZ

The current task explores automatic generation control knowledge under old-style circumstances for a triple-arena scheme. Sources in area-1 are thermal-solar thermal (ST); thermal-geothermal power plant (GPP) in area-2 and thermal-hydro in area-3. An original endeavour has been set out to execute a new performance index named hybrid peak area integral squared error (HPA-ISE) and two-stage controller with amalgamation of proportional-integral and fractional order proportional-derivative, hence named as PI(FOPD). The performance of PI(FOPD) has been compared with varied controllers like proportional-integral (PI), proportional-integral-derivative (PID). Various investigation express excellency of PI(FOPD) controller over other controller from outlook regarding lessened level of peak anomalies and time duration for settling. Thus, PI(FOPD) controller's excellent performance is stated when comparison is undergone for a three-area basic thermal system. The above said controller's gains and related parameters are developed by the aid of Artificial Rabbit Optimization (ARO). Also, studies with HPA-ISE enhances system dynamics over ISE. Moreover, a study on various area capacity ratios (ACR) suggests that high ACR shows better dynamics. The basic thermal system is united with re-

A. Saha (e-mail: sahaarindita.91@gmail.com) is with Department of Electrical Engineering, Regent Education & Research Foundation Group of Institutions, Kolkata, West Bengal, India.

T. Chiranjeevi (e-mail: tirumalasetty.chiranjeevi@recsonbhadra.ac.in) is with Department of Electrical Engineering, Rajkiya Engineering College Sonbhadra, U.P., India.

R. Devarapalli (e-mail: Dr.R.Devarapalli@gmail.com) is with Institute of Chemical Technology, Indian Oil Odisha Campus, Bhubaneswar, India.

N.R. Babu (e-mail: rambabu.nits@yahoo.com) is with Department of Electrical & Electronics Engineering, Aditya Engineering College, Surampalem, Andhra Pradesh, India.

P. Dash (e-mail: pujadash.nits@gmail.com) is with Department of Electrical and Electronics Engineering, Gayatri Vidya Parishad College of Engineering (Autonomous), Visakhapatnam, Andhra Pradesh, India.

F.P.G. Márquez (corresponding author, e-mail: FaustoPedro.Garcia@uclm.es) is with Ingenium Research Group, University of Castilla-La Mancha, Spain.

Received 21.01.2023.

newable sources ST in area-1 also GPP in area-2. Also, hydro unit is installed in area-3. The performance of this new combination of system is compared with the basic thermal system using PI(FOPD) controller. It is detected that dynamic presentation of new system is improved. Action in existence of redox flow battery is also examined which provides with noteworthy outcome. PI(FOPD) parameters values at nominal condition are appropriate for higher value of disturbance without need for optimization.

Key words: solar thermal, automatic generation control, geothermal, artificial rabbit optimization, redox flow battery, PI(FOPD) controller

1. Introduction

A balance between an amount of power generated and loss is the basic need of power system. This balance is very difficult to obtain during high peak periods. The mismatch reflects in the frequency and tie-line powers. If these discrepancies persist for long time, then it leads to huge damage. These disparities are overcome by the concept of automatic generation control (AGC).

Authors in [1,2] has implemented the numerical prototype of AGC. In earlier times, utmost number of works were restricted to solo area scheme. Subsequently, the works were passed frontward for manifold arenas like two area, three areas. Golpria *et al.* [3] has undertaken scrutiny of a three-arena thermal scheme. Authors in [4] has considered a two-arena scheme comprising of hydro and thermal as generating units. The main source of electricity generation is fossil fuels. But constant use of fossil fuel is depleting the natural resource and hampering the environment by constant boiling. This demands for the usage of sustainable causes like solar, geothermal, and wind. Works obtainable in the arena of AGC knowledge reflects the usage of solar, wind and geothermal. Sharma *et al.* [5], stated the practice of solar in the learning of AGC. Saha *et al.* [6] stretched their effort for reorganized scheme with enclosure of solar. Tasnin *et al.* [7] have exploited geothermal in study of traditional AGC learning. Very few literatures point out the usage of solar and geothermal together. Thus, it is of great opportunity to undergo AGC knowledge with multiple sources in multiple arenas along with sustainable sources. Further, system stabilization can be further achieved by incorporation of energy storing devices (ESD). AGC learning reflects about the usage of redox flow battery (RFB) [8]. Thus, the system combination with RFB calls for further studies.

The main intention of AGC is towards declining the anomaly to zero for both frequency and interlinking power of areas. To consummate this determination, supplementary controllers are employed. In the learning of AGC various diverse varieties of controller alike fractional order (FrO) [9], integral order (InO), higher order, two-step controllers are stated in literature. The InO controllers alike integral (I) [3,10], PI [4,11], PID [5,12,13], integral-derivative with filter (IDF) [14] by now find their usage in the learning of AGC. Advanced order subordinate

controllers like dual-degree of freedom (dof), triple dof [15, 16] and fuzzy subordinate controllers [16] are too applied in AGC. The knowledge in AGC works call attention to the procedure of InO order two-stage controllers PI-PD [17], FrO two-stage controllers FOPI-FOPD [7], as well amalgamation of InO and FrO controllers PIDN-FOPD [6], IDN-FOPD [8]. But series cascade combination of PI with FrO proportional-derivative termed as FOPD has not been so far specified in AGC works. Furthermore, usage of PI(FOPD) controller in the triple-area solar thermal-geothermal-hydro-thermal scheme has not been conveyed beforehand, so claims the necessity of examination.

The literature proclaims about the practice of diverse optimization practices. These methods are necessary for satisfactory alteration of controller gains and related parameters. The methods of diverse categories like conventional and evolutionary procedures (EAm) [18–21]. The conventional method is circumvented as the method is very chaotic and deliver bad outcomes as they experience prospect of getting wedged in limited targets. EAm are unrestricted from the drawbacks of conventional method. Several EAm find their relevance in the arena of AGC. Some of them are genetic algorithm (GA) [3], firefly algorithm (FA) [12, 14, 22], whale optimization algorithm (WOA) [6], sine-cosine algorithm (SCA) [7], biogeography-based algorithm (BBO) [16], ant-lion optimizer (ALO) [13], bacterial foraging-based optimization technique (BFO) [10], grey wolf optimizer (GWO) [23]. Wang *et al.* [24] have recently evolved an optimization strategy named as artificial rabbit optimization (ARO). ARO has evolved after being inspired by living tactics of rabbits in nature. Moreover, ARO method has employed in AGC structure with solar thermal, geothermal, hydro, thermal elements. This gives propositions of forthcoming valuations.

Regarding the above statements, intents of work are:

- To establish a triple-arena thermal scheme.
- To evaluate structural dynamics of scheme stated with diverse controllers like PI, PID and PD(FOPI) with ARO to attain the superlative controller.
- Evaluate scheme dynamics by superlative controller attained by the practice of diverse algorithms like FA, GWO, and ARO to realize the topmost optimization method.
- To evaluate scheme dynamics in existence of solar thermal, geothermal and hydro elements with superlative controller besides algorithm.
- Evaluate scheme dynamic execution with amalgamation of RFB.
- Undertake sensitivity valuation with superlative controller in consideration of changed step load disturbance.

2. System investigated

The system under consideration is a three-area system which encompasses solar thermal-thermal units in arena-1, geothermal-thermal units in arena-2, hydrothermal units in arena-3 along with energy storage device RFB in all areas. The area capacity ratio considered is 1:3:5. The thermal unit is associated with non-linearity generate rate constraint (GRC) of 3% per minute. The participation factors (pf) of each generating units of respective areas are as $pf_{11} = 0.2$, $pf_{12} = 0.8$ in area-1, $pf_{21} = 0.25$, $pf_{22} = 0.75$ in area-2 and $pf_{31} = 0.3$, $pf_{32} = 0.7$ in area-3.

Geothermal energy is a potential renewable source of energy where underground thermal energy is transformed into electricity. The transfer function modelling of GPP is similar to thermal plants but it does not have the boiler for reheating steam. The first order transfer function of governor and turbine of GPP are given by (1) and (2) respectively.

$$G_{\mathrm{GPP}} = \frac{1}{1 + sg_{21}}, \tag{1}$$

$$T_{\mathrm{GPP}} = \frac{1}{1 + st_{21}}, \tag{2}$$

g_{21} and t_{21} are the time constants of governor and turbine of GPP respectively. These values are obtained by optimization technique ARO within the prescribed limits.

Redox flow battery is category of drift battery, established on the base of motionless energy stowing practices. RFB has initiated great numeral of utilization in the arena of AGC. Here, the reactive substantive is missing in the construction relatively it is assisted from an exterior establishment of stowage containers. Hence, the entire energy competence is reliant on the measure of electrolyte inside exterior stowage reservoirs and power yield is linked to the association of electrodes. Blend of sulfuric acid in grouping through vanadium ions is considered as the electrolyte. A duo of drives is related to movement the solution by virtue of cells (electrochemical type) of battery. Electrochemical reactions whichever arise internal battery electrochemical cell throughout charging with discharging are specified by (3)–(4).

At site of +ve electrical conductor:

$$V^{4+} \overset{\text{Charge Discharge}}{\rightleftarrows} V^{5+} + e^{-}. \tag{3}$$

At site of −ve electrical conductor:

$$V^{3+} + e^{-} \overset{\text{Charge Discharge}}{\rightleftarrows} V^{2+} \tag{4}$$

RFB is stated with prosperity of elongated operational duration and eases with huge power capacity. Even has secure profits like quick small-span additional ability, huge efficiency, exposed from autonomous-discharge matters, inexpensive, not cluttered by unforeseen charging or discharging.

The transfer function prototype of scheme is manifested in Fig. 1. The minimal values of scheme limitations are specified in Addendum. The premium standards of controller gains and related constraints are accomplished by the assistance of by artificial rabbit optimization usage of HPA-ISE as the essential performance index ($J_{HPA-ISE}$) [25, 26] revealing to 1% step load disturbance (SLP) at position of area-1 is stated by (5).

$$J_{\text{HPA-ISE}} = \int_{o}^{t} \left((\Delta f_i)^2 + (\Delta P_{tiei-j})^2 + \left|\Delta f_{i,\text{peak}}\right| + \left|\Delta P_{tiei-j\text{peak}}\right| \right) \mathrm{d}t \,. \tag{5}$$

Here, i and j are number of areas, $i = 1,\ 2,\ 3$ and $i \neq j$.

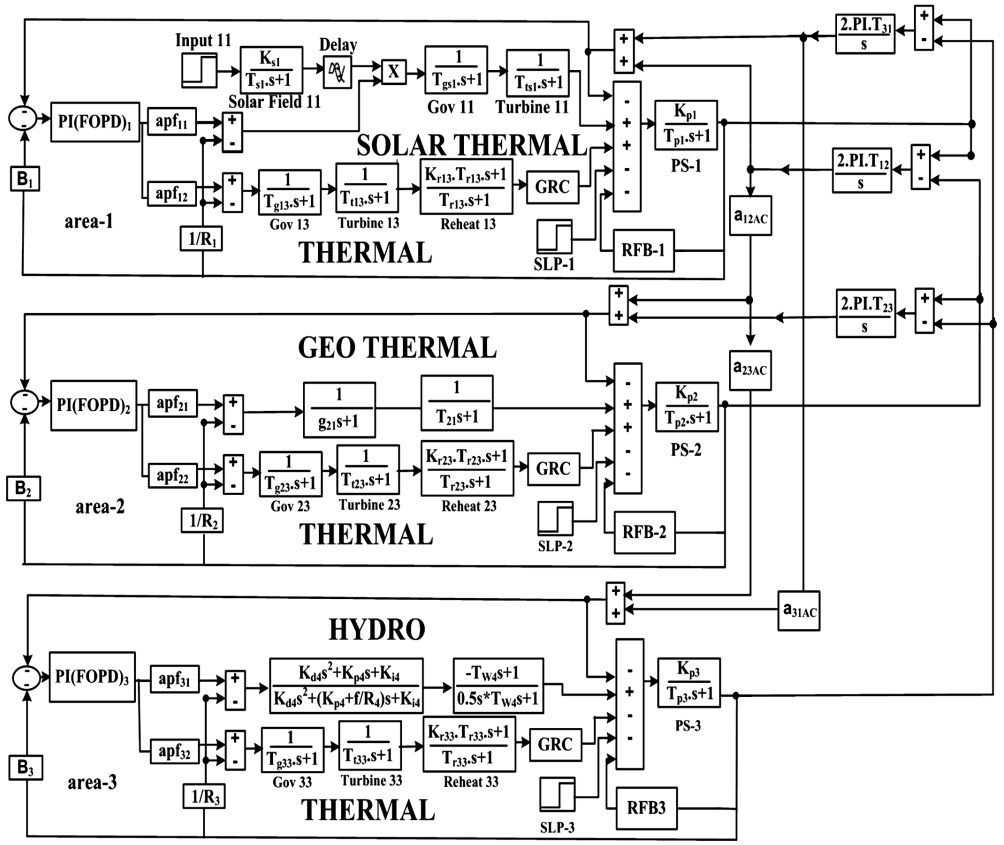

Figure 1: Transfer function (Trfn) structure of three-area multiple source scheme including energy storage device RFB

3. The proposed PI(FOPD) controller

The commended controller is aggregate of InO together with FrO controllers. Commended controller is InO proportional-integral (PI) with FrO proportional-derivative (FOPD), hence PI(FOPD). Arrangement of PI(FOPD) is substantiated in Fig. 2. Segment-1 (B1) and Segment-2 (B2) are layout of PI and FOPD one-to-one. $\mathrm{Rs}_i(\mathrm{s})$ is the antecedent signal and $\mathrm{Os}_i(\mathrm{s})$ is the outcome signal for PI(FOPD) controller. The Trfn of $\mathrm{B1}_i(\mathrm{s})$ is manifested by (6).

$$\mathrm{Trfn}_{(PI)i} = K_{P_i} + K_{Ii}/s. \tag{6}$$

InO proportional gain is symbolized as $\mathrm{K_{Pi}}$ and integral gain as $\mathrm{K_{Ii}}$ for i-th suggested area.

Summarization of Riemann-Liouville for FrO derivative is obtainable from (7) [29, 30].

$$\begin{gathered} {}^{\alpha}D_t^{\alpha} f(t) = \frac{1}{\Gamma(n-\alpha)} \frac{d^n}{dt^n} \int_{\alpha}^{t} (t-\tau)^{n-\alpha-1} f(\tau)\,\mathrm{d}\tau, \\ n-1 < \alpha < n, \quad n \text{ is an integer}, \end{gathered} \tag{7}$$

${}^{\alpha}D_t^{\alpha}$ – fractional operator, $\Gamma(.)$ – Euler's gamma function. The alteration of Fro derivative in Laplace domain is given by (8).

$$L\left\{{}^{\alpha}D_t^{\alpha} f(t)\right\} = s^{\alpha}F(s) - \sum_{k=0}^{n-1} s^{k\alpha} D_t^{\alpha-k-1} f(t)\big|_{t=0}. \tag{8}$$

The detriment of boundless computation of poles and zeros by virtue of absolute resemblance is manifested by Oustaloup *et al.* [31]. Here a convenient Trfn is propounded which can be approximated FrO derivatives together with integrators by dint of recursive distribution around poles and zeros substantiated by (9).

$$s^{\alpha} = K \prod_{n=1}^{M} \frac{1 + \left(\dfrac{s}{\omega_{Z,n}}\right)}{1 + \left(\dfrac{s}{\omega_{p,n}}\right)}. \tag{9}$$

Suppose attuned gain $K = 1$, gain = 0 dB through 1 rad/s frequency, M – count of poles along with zeros (fixed beforehand) and frequencies choice for poles and zeros are manifested by (10)–(14).

$$\omega_{Z,l} = \omega_l \sqrt{n}\,, \tag{10}$$

$$\omega_{p,n} = \omega_{Z,n}\varepsilon, \quad n = 1, \ldots, M, \tag{11}$$

$$\omega_{Z,n+1} = \omega_{p,n}\sqrt{\eta}, \tag{12}$$

$$\varepsilon = \left(\frac{\omega_h}{\omega_l}\right)^{v/M}, \tag{13}$$

$$\eta = \left(\frac{\omega_n}{\omega_l}\right)^{(1-v)/M}. \tag{14}$$

The Trfn for FOPD is given by (15).

$$\text{Trfn}_{(\text{FOPD})i} = (K_{KP})_i + (K_{KD})_i s^{\mu_i}. \tag{15}$$

The Trfn for PI(FOPD) controller is shown in (16).

$$\text{Trfn}_{\text{PI(FOPD)}i} = (K_{Pi} + K_{Ii}/s) \times (K_{KP})_i + (K_{KD})_i s^{\mu_i}. \tag{16}$$

The Trfn demonstration of cascade PI(FOPD) controller is in Fig. 2. Commended PI(FOPD) controller gains are boosted by ARO with margins in (17).

$$\begin{gathered} 0 \leqslant K_{Pi} \leqslant 1, \qquad 0 \leqslant K_{Ii} \leqslant 1, \\ 0 \leqslant K_{KPi} \leqslant 1, \quad 0 \leqslant K_{KDi} \leqslant 1 \quad \text{and} \quad 0 \leqslant \mu_i \leqslant 1. \end{gathered} \tag{17}$$

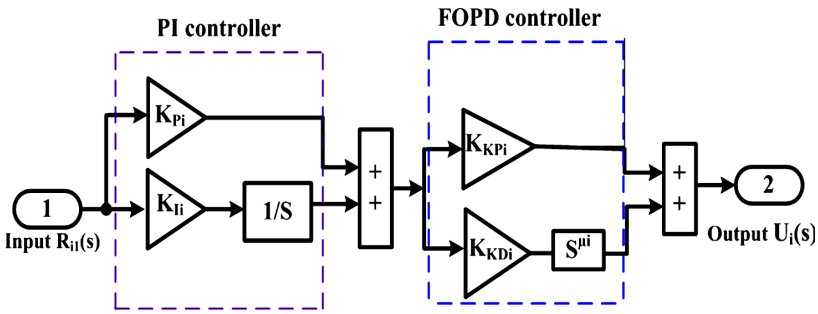

Figure 2: Prototypical of PI(FOPD) controller

4. Optimization technique-ARO

The ARO has evolved from the existence tactics of rabbit in wildlife. The ARO has been developed by Wang *et al.* [24] after being inspired by two important features alike, rabbits hunt for meal distant from their shells and other one is arbitrary shelter. ARO engage the rummaging and hiding approaches of actual rabbits, along with their energy constriction leading to conversion amid both approaches.

1. Detour foraging i.e., exploration: Since, rabbits look for food away from their own shelter so, in ARO it is considered that each of the rabbits has its own arena with food and d number of holes. And, each rabbit moves arbitrarily to other member's arenas for the hunt of food. The numerical prototype of the exploration of each rabbit is as follows:

$$\vec{v}_i(t+1) = \vec{x}_j(t) + R \cdot (\vec{x}_i(t) - \vec{x}_j(t)) + \text{round}(0.5 \cdot (0.05 + r_1)) \cdot n_1$$
$$i,\ j = 1, \ldots, n \quad \text{and} \quad i \neq j$$
where
$\vec{v}_i(t+1) \Rightarrow$ Candidate location of i-th rabbit at $(t+1)$ time
$\vec{x}_i(t) \Rightarrow$ Location of i-th rabbit at (t) time
$n \Rightarrow$ Size of rabbit population
$R \Rightarrow$ Runing operator
$\cdot \Rightarrow$ Ceiling function
round $\Rightarrow$ Rounding to nearest integer
$r_1 \Rightarrow$ Random number in between (01)
$n_1 \Rightarrow$ Subject to the standard normal distribution (18)

$$R = L \cdot c$$
where
$L \Rightarrow$ Running length
$c \Rightarrow$ Mapping vector (19)

$$L = \left(e - e^{\left(\frac{t-1}{T}\right)^2}\right) \sin(2\pi r_2)$$
where
$r_2 \Rightarrow$ Random number in between (0, 1) (20)

$$c(k) = \begin{cases} 1 & \text{if } k == g(l) \\ 0 & \text{else} \end{cases} \qquad k = 1, \ldots, d \text{ and } l = 1, \ldots, \lceil r_3 d \rceil$$
where
$d \Rightarrow$ Dimension of the problem
$r_3 \Rightarrow$ Random number in (0, 1) (21)

$$g = \text{randperm}(d)$$
where
randperm $\Rightarrow$ returns a random permutation of the integers from 1 to d (22)
$n_1 \sim N(0,\ 1)$. (23)

2. Arbitrary hiding i.e., exploitation: In the present ARO, at individual repetition, a rabbit constantly produces d hideaways about it along individual dimension of the hunt area, and it continually arbitrarily selects single from all holes for hiding to lessen the likelihood of being hunted. Here, the j-th hole of the i-th rabbit

is engendered by:

$$\vec{b}_{i,j}(t) = \vec{x}_i(t) + H \cdot g \cdot \vec{x}_i(t), \quad i = 1, \ldots, n \text{ and } j = 1, \ldots, d$$

where

$$H \Rightarrow \text{Hiding parameter} \tag{24}$$

$$H = \frac{T - t + 1}{T} r_4$$

where

$$r_4 \Rightarrow \text{Random number in between (0, 1)} \tag{25}$$

$$n_2 \sim N(0,\ 1) \tag{26}$$

$$g(k) = \begin{cases} 1 & \text{if } k == j \\ 0 & \text{else} \end{cases} \qquad k = 1, \ldots, d. \tag{27}$$

The equations needed to develop numerical prototype for arbitrary hiding approach is as:

$$\vec{v}_i(t+1) = \vec{x}_i(t) + R \cdot (r_4 \vec{b}_{i,r}(t) - \vec{x}_i(t)), \quad i = 1, \ldots, n$$

where

$\vec{b}_{i,r}(t) \Rightarrow$ Randomly chosen burrow for hiding from its d burrows

$r_4 \Rightarrow$ Random number in (0, 1). (28)

After one complete process of exploration and exploitation, the spot of rabbit is updated by

$$\vec{x}_i(t+1) = \begin{cases} \vec{x}_i(t) & f(\vec{x}_i(t) \leqslant f(\vec{v}_i(t+1)) \\ \vec{v}_i(t+1) & f(\vec{x}_i(t)) > f(\vec{v}_i(t+1)). \end{cases} \tag{29}$$

3. Energy constriction i.e. change from exploration to exploitation: The rabbits have the nature to undergo exploration in the first phase followed by exploitation in the next phase. This difference in search is due to the loss of energy in rabbits in due course of time. This energy matter is designed by the following expression.

$$A(t) = r \left(1 - \frac{t}{T}\right) \ln \frac{1}{r}. \tag{30}$$

The flow diagram of ARO is in Fig. 3.

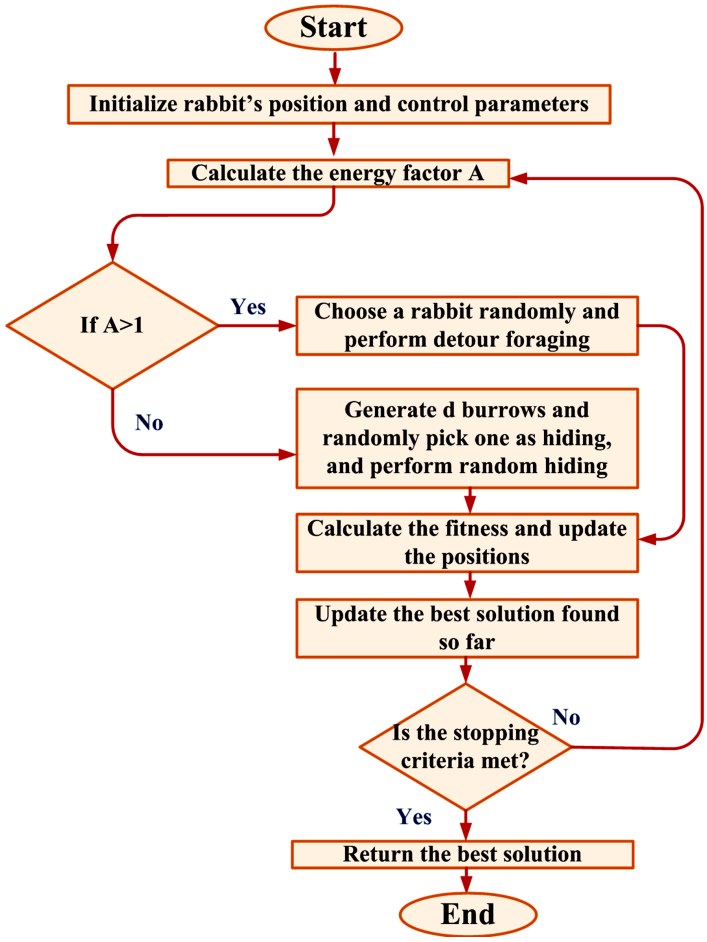

Figure 3: Flowchart of ARO

5. Outcomes and valuation

5.1. Valuation of Scheme Outcomes through Several Controllers alike PI, PID and PI(FOPD)

A trio-area thermal scheme is engaged for valuation. The ACR of the contemplated scheme is 1:3:5. The scheme is entitled with diverse controllers like PI, PID and the projected PI(FOPD) controller on individual basis with HPA-ISE as performance index. The premium standards of subordinate controller gains and related constraints are accomplished employing ARO and the numerical values are manifested in Table 1a. Potent frequency outcomes are exposed in Figure 4a–4b. Tie-line power deflection outcome are manifested in Figure 4c–4d. The values of peak anomaly (Pk_O, Pk_U) and settling_time (S_Time) are

looked out in Table 1b. The responses of Figure 4 and values of Table 1b shows the clarity of superior performance of PI(FOPD) controller in terms of Pk_O, Pk_U and S_Time.

Table 1

(a) ARO optimized gains and related parameters of subordinate controllers considering HPA-ISE (thermal system only)

PI	$K_{P1(PI)} = 0.0621$	$K_{I1(PI)} = 0.5607$	$K_{P2(PI)} = 0.0591$
	$K_{I2(PI)} = 0.5861$	$K_{P3(PI)} = 0.0461$	$K_{I3(PI)} = 0.5868$
PID	$K_{P1(PID)} = 0.5650$	$K_{I1(PID)} = 0.7586$	$K_{D1(PID)} = 0.1642$
	$K_{P2(PID)} = 0.5324$	$K_{I2(PID)} = 0.7768$	$K_{D2(PID)} = 0.1721$
	$K_{P3(PID)} = 0.6133$	$K_{I3(PID)} = 0.7768$	$K_{D3(PID)} = 0.1831$
PI(FOPD)	$K_{P1(PI(FOPD))} = 0.0004$	$K_{I1(PI(FOPD))} = 0.3489$	$K_{KP1(PI(FOPD))} = 0.0018$
	$K_{KD1(PI(FOPD))} = 0.9963$	$\mu_{1(PI(FOPD))} = 0.0090$	$K_{P2(PI(FOPD))} = 0.0036$
	$K_{I2(PI(FOPD))} = 0.1271$	$K_{KP2(PI(FOPD))} = 0.0005$	$K_{KD2(PI(FOPD))} = 0.9160$
	$\mu_{2(PI(FOPD))} = 0.0089$	$K_{P3(PI(FOPD))} = 0.0012$	$K_{I3(PI(FOPD))} = 0.1367$
	$K_{KP3(PI(FOPD))} = 0.0017$	$K_{KD3(PI(FOPD))} = 0.9508$	$\mu_{3(PI(FOPD))} = 0.0041$

(b) Evaluation of dynamic outcomes with respect to different characteristics using varied controllers

Characteristics		PI	PID	PI(FOPD)
Δf_1	Pk_O	0.0168	0.0159	0.0077
	Pk_U	0.0289	0.0304	0.0275
	S_Time	Not settling	70.00 sec	60.00 sec
Δf_2	Pk_O	0.0146	0.0106	0.0036
	Pk_U	0.0261	0.0260	0.0241
	S_Time	Not settling	73.54 sec	65.56 sec
$\Delta Ptie_{2-3}$	Pk_O	0.0017	0.0013	0.0011
	Pk_U	0.0035	0.0034	0.0032
	S_Time	Not settling	71.44 sec	67.36 sec
$\Delta Ptie_{1-3}$	Pk_O	0.0010	0.0006	0.0005
	Pk_U	0.0085	0.0085	0.0082
	S_Time	Not settling	67.53 sec	62.55 sec

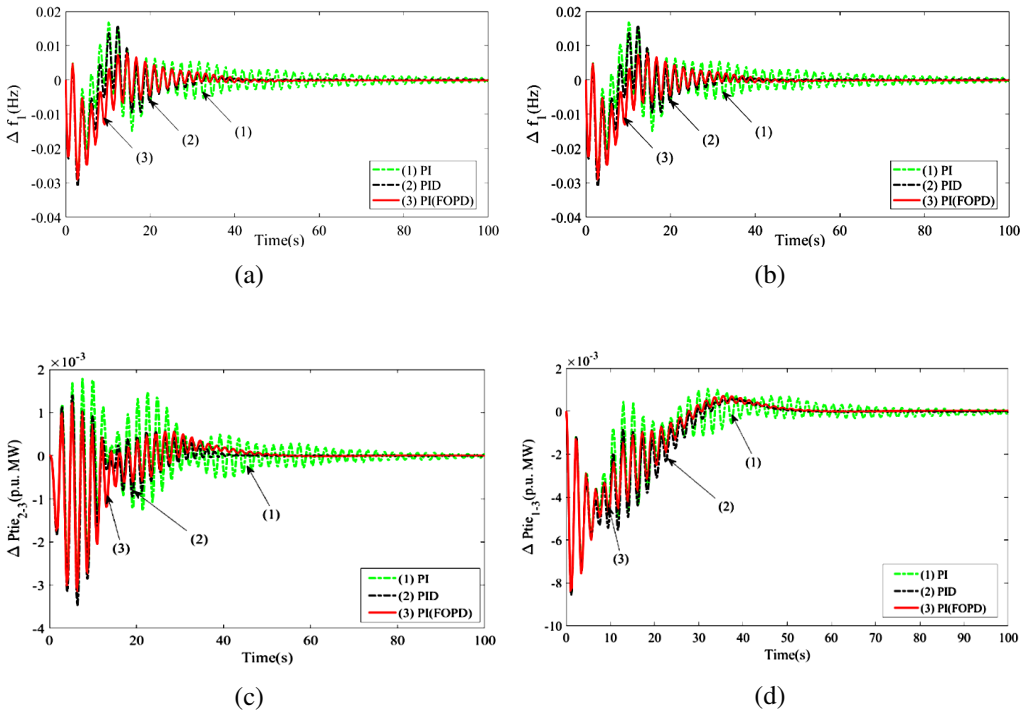

Figure 4: Diagram of deflection in dynamic observation of the thermal scheme employing subordinate controllers contrast time: (a) Deflection of frequency observation of arena-1, (b) Deflection of frequency observation of arena-2, (c) Deflection in tie-line power interlinking arena-2 and arena-3, (d) Deflection in tie-line power interlinking arena-1 and arena-3

5.2. Evaluation of Scheme Outcomes for Diverse Algorithms In view of PI(FOPD) Controller and HPA-ISE

Preceding sub-segment specifies that PI(FOPD) subordinate controller is the finest attained controller. Presently, in current sub-segment PI(FOPD) subordinate controller is once more augmented employing not many algorithms alike FA, GWO, ARO in view of HPA-ISE as performance index. The finest values of the controller gains in addition related constraints employing the above-mentioned algorithms are manifested in Table 2a. The potent observation accomplished are acknowledged in Figure 5a–5d. Contrasting convergence curvature is furnished in Figure 5e. Thorough examination of Figure 5a–5d demonstrate that potent observation employing ARO optimized subordinate controller delivers enhanced outcomes. Subsequently, observation of ARO optimized controller illustrates diminished amount of Pk_O, Pk_U and S_Time. Correspondingly, the conver-

gences curvature replicated in Figure 5e with corresponding $J_{HPA-ISE}$ in Table 2b states that ARO converges more rapidly than further contemplated optimization approaches.

Table 2

(a) Gains and related parameters of PI(FOPD) controller employing diverse algorithm alike FA, GWO and ARO in view of HPA-ISE (thermal system only)

FA	$K_{P1(PI(FOPD))} = 0.0188$	$K_{I1(PI(FOPD))} = 0.7563$	$K_{KP1(PI(FOPD))} = 0.0065$
	$K_{KD1(PI(FOPD))} = 0.5543$	$\mu_{1(PI(FOPD))} = 0.0045$	$K_{P2(PI(FOPD))} = 0.0164$
	$K_{I2(PI(FOPD))} = 0.7768$	$K_{KP2(PI(FOPD))} = 0.0038$	$K_{KD2(PI(FOPD))} = 0.5646$
	$\mu_{2(PI(FOPD))} = 0.0034$	$K_{P3(PI(FOPD))} = 0.0178$	$K_{I3(PI(FOPD))} = 0.8765$
	$K_{KP2(PI(FOPD))} = 0.0168$	$K_{KD2(PI(FOPD))} = 0.5432$	$\mu_{2(PI(FOPD))} = 0.0065$
GWO	$K_{P1(PI(FOPD))} = 0.0176$	$K_{I1(PI(FOPD))} = 0.7563$	$K_{KP1(PI(FOPD))} = 0.0061$
	$K_{KD1(PI(FOPD))} = 0.5121$	$\mu_{1(PI(FOPD))} = 0.0043$	$K_{P2(PI(FOPD))} = 0.0175$
	$K_{I2(PI(FOPD))} = 0.7346$	$K_{KP2(PI(FOPD))} = 0.0041$	$K_{KD2(PI(FOPD))} = 0.6066$
	$\mu_{2(PI(FOPD))} = 0.0043$	$K_{P3(PI(FOPD))} = 0.0615$	$K_{I3(PI(FOPD))} = 0.8565$
	$K_{KP3(PI(FOPD))} = 0.0187$	$K_{KD3(PI(FOPD))} = 0.4321$	$\mu_{2(PI(FOPD))} = 0.0071$

(b) Valuation of dynamic Outcome with regard to diverse features using wide-ranging algorithms

Characteristics		FA	GWO	ARO
Δf_1	Pk_O	0.0147	0.0128	0.0077
	Pk_U	0.0285	0.0283	0.0275
	S_Time	64.34 sec	63.66 sec	60.00 sec
Δf_2	Pk_O	0.0122	0.0097	0.0036
	Pk_U	0.2431	0.2422	0.0241
	S_Time	81.51 sec	74.88 sec	65.56 sec
$\Delta Ptie_{2-3}$	Pk_O	0.0014	0.0015	0.0011
	Pk_U	0.0034	0.0035	0.0032
	S_Time	78.14 sec	73.58 sec	67.36 sec
$\Delta Ptie_{1-3}$	Pk_O	0.0008	0.0006	0.0005
	Pk_U	0.0087	0.0084	0.0082
	S_Time	78.55 sec	76.81 sec	62.55sec
$J_{HPA-ISE}$		0.0068	0.0070	**0.0067**

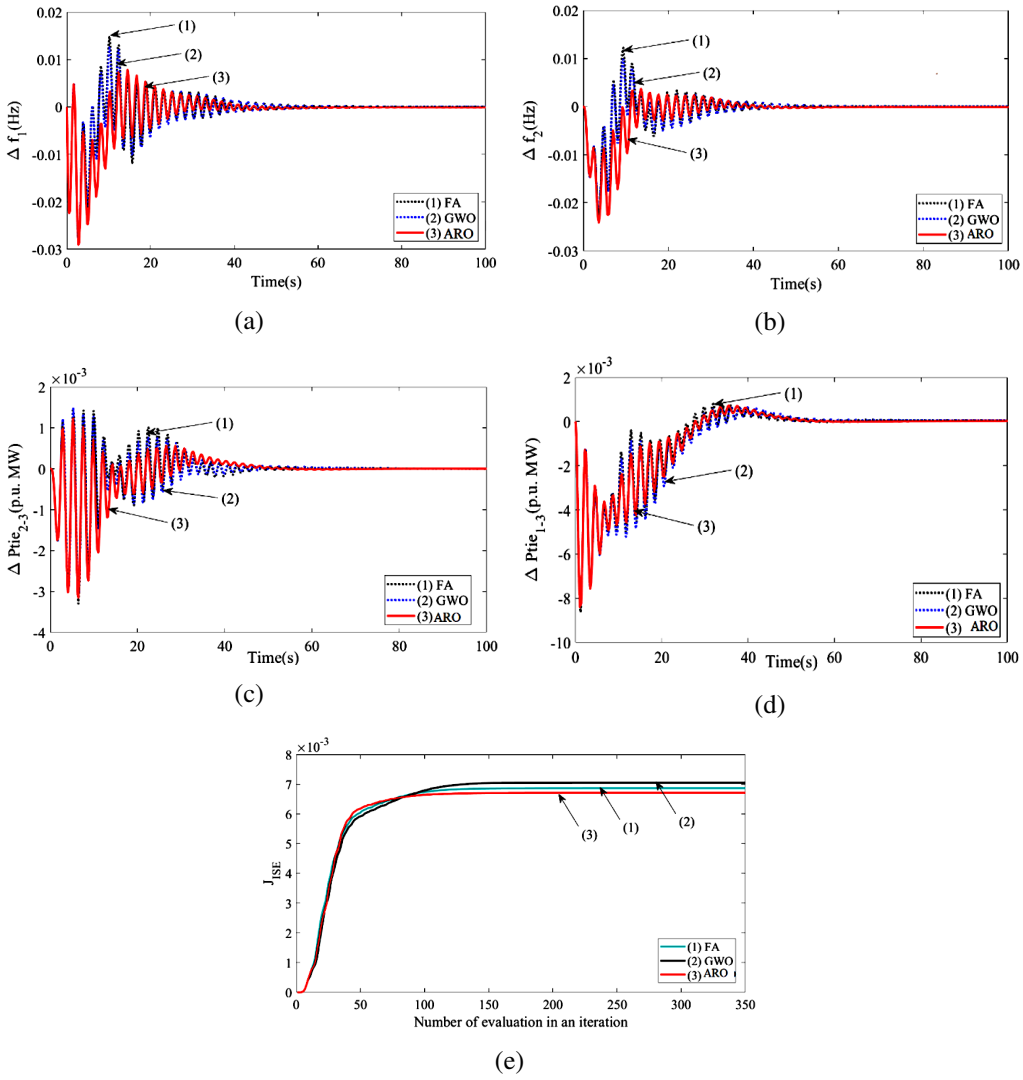

Figure 5: Diagram of deflection in potent observation and convergence curvature for diverse schemes alike FA, GWO and ARO via PI(FOPD) subordinate controller contrast time: (a) Deflection of frequency observation of arena-1, (b) Deflection of frequency observation of arena-2, (c) Deflection in tie-line power interlinking arena-2 and arean-3, (d) Deflection in tie-line power interlinking arena-1 and arena-3, (e) Contrasting Convergence curvature

5.3. Contrast of scheme dynamics for various area capacity ratios (ACR)

This study is carried to identify the effect of various ACRs on the system in Section 5.2. Various ACRs such as 1:1:1, 1:2:3 and 1:2:4 are deliberted for the

study. The investigated is system with three ACRs is subjected to of PI(FOPD) controller, whose gains are optimized by ARO controller considering HPA-ISE as performance index. The obtained optimum values are noted in Table 3 and the obtained responses are compared with response for system with ACR 1:3:5 and plotted in Figure 6. From Figure 6; it is noted that as the ACR rises, the system ehibits enhaced responses interms of Pk_O, Pk_U and S_Time.

Table 3: Outstanding gains and correlated parameters of PI(FOPD) subordinate controller via varied various ACRs

ACR = 1:1:1	$K_{P1(PI(FOPD))} = 0.0178$	$K_{I1(PI(FOPD))} = 0.7763$	$K_{KP1(PI(FOPD))} = 0.0075$
	$K_{KD1(PI(FOPD))} = 0.5453$	$\mu_{1(PI(FOPD))} = 0.0044$	$K_{P2(PI(FOPD))} = 0.0144$
	$K_{I2(PI(FOPD))} = 0.7457$	$K_{KP2(PI(FOPD))} = 0.0034$	$K_{KD2(PI(FOPD))} = 0.5647$
	$\mu_{2(PI(FOPD))} = 0.0035$	$K_{P3(PI(FOPD))} = 0.0165$	$K_{I3(PI(FOPD))} = 0.8546$
	$K_{KP3(PI(FOPD))} = 0.0015$	$K_{KD3(PI(FOPD))} = 0.5546$	$\mu_{3(PI(FOPD))} = 0.0066$
ACR = 1:2:3	$K_{P1(PI(FOPD))} = 0.0165$	$K_{I1(PI(FOPD))} = 0.7546$	$K_{KP1(PI(FOPD))} = 0.0046$
	$K_{KD1(PI(FOPD))} = 0.5643$	$\mu_{1(PI(FOPD))} = 0.0063$	$K_{P2(PI(FOPD))} = 0.0165$
	$K_{I2(PI(FOPD))} = 0.7453$	$K_{KP2(PI(FOPD))} = 0.0034$	$K_{KD2(PI(FOPD))} = 0.5543$
	$\mu_{2(PI(FOPD))} = 0.0034$	$K_{P3(PI(FOPD))} = 0.0146$	$K_{I3(PI(FOPD))} = 0.8554$
	$K_{KP3(PI(FOPD))} = 0.0015$	$K_{KD3(PI(FOPD))} = 0.5676$	$\mu_{3(PI(FOPD))} = 0.0065$
ACR = 1:2:4	$K_{P1(PI(FOPD))} = 0.0163$	$K_{I1(PI(FOPD))} = 0.7455$	$K_{KP1(PI(FOPD))} = 0.0045$
	$K_{KD1(PI(FOPD))} = 0.6545$	$\mu_{1(PI(FOPD))} = 0.0054$	$K_{P2(PI(FOPD))} = 0.0234$
	$K_{I2(PI(FOPD))} = 0.6879$	$K_{KP2(PI(FOPD))} = 0.0044$	$K_{KD2(PI(FOPD))} = 0.6436$
	$\mu_{2(PI(FOPD))} = 0.0065$	$K_{P3(PI(FOPD))} = 0.0234$	$K_{I3(PI(FOPD))} = 0.6345$
	$K_{KP3(PI(FOPD))} = 0.0032$	$K_{KD3(PI(FOPD))} = 0.7698$	$\mu_{3(PI(FOPD))} = 0.0045$

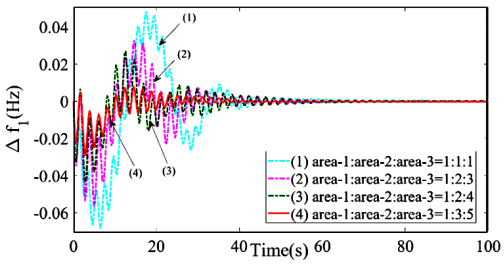

(a)

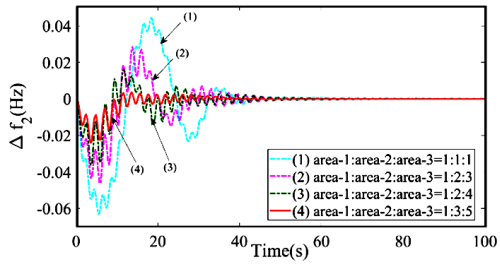

(b)

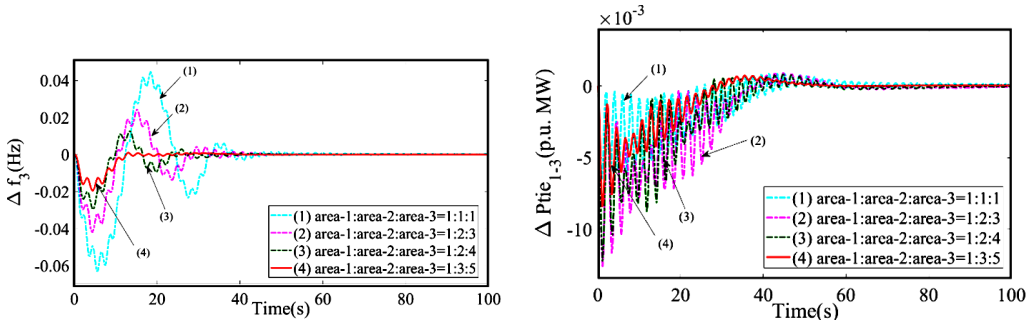

(c) (d)

Figure 6: Dynamic response comparison with different ACR contrast time (a) Arena-1 frequency anomaly, (b) Arena-2 frequency anomaly, (c) Arena-3 frequency anomaly, (d) Tie-power anomaly amid arena_1 and arena-3

5.4. System dynamic valuation among ISE and HPA-ISE

Scheme in segment-5.3 is provided with PI(FOPD) controller considering ISE as performance index and gains are optimized by ARO technique. The obtained optimum values with ISE are noted Table 4 and the responses with ISE are compared with he obtained results from Section 5.3 (i.e., with HPA-ISE) and are plotted in Figure 7. Observations suggests that results with HPA-ISE outperforms over ISE.

Table 4: Gains and other parameters of PI(FOPD) controller considering ISE as a performance index

ACR = 1:3:5	$K_{P1(PI(FOPD))} = 0.0188$	$K_{I1(PI(FOPD))} = 0.7563$	$K_{KP1(PI(FOPD))} = 0.0065$
	$K_{KD1(PI(FOPD))} = 0.5543$	$\mu_{1(PI(FOPD))} = 0.0045$	$K_{P2(PI(FOPD))} = 0.0164$
	$K_{I2(PI(FOPD))} = 0.7768$	$K_{KP2(PI(FOPD))} = 0.0038$	$K_{KD2(PI(FOPD))} = 0.5646$
	$\mu_{2(PI(FOPD))} = 0.0034$	$K_{P3(PI(FOPD))} = 0.0178$	$K_{I3(PI(FOPD))} = 0.8765$
	$K_{KP3(PI(FOPD))} = 0.0168$	$K_{KD3(PI(FOPD))} = 0.5432$	$\mu_{3(PI(FOPD))} = 0.0065$

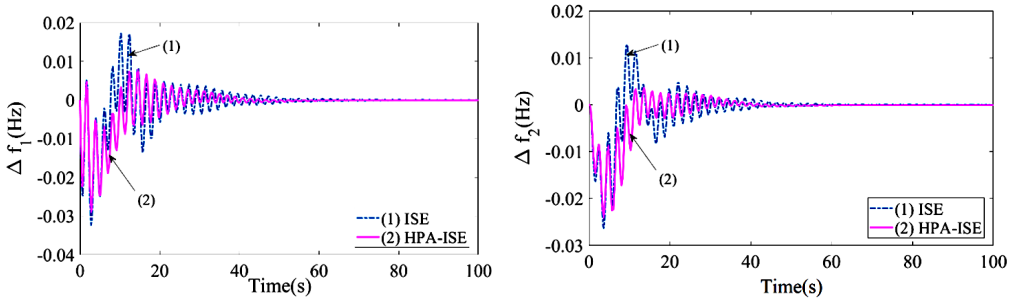

(a) (b)

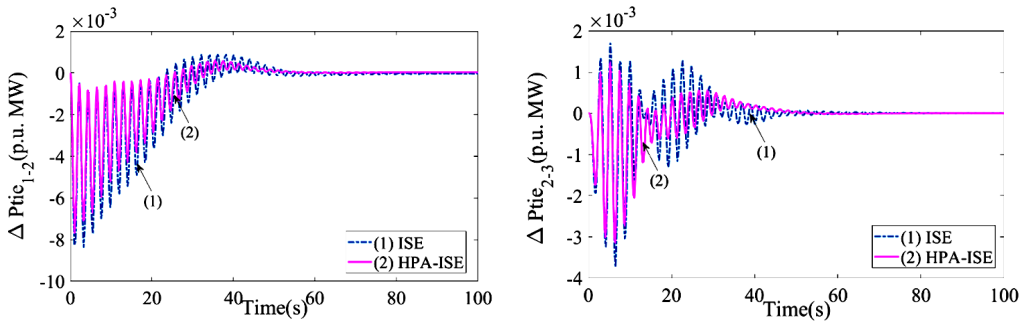

Figure 7: System dynamic response comparison among ISE and HPA-ISE contrast time: (a) Arena-1 frequency anomaly, (b) Arena-2 frequency anomaly, (c) Tie-power anomaly amid arena-1 and arena-2, (d) Tie-power anomaly amid arena-2 and arena-3

5.5. Valuation of scheme dynamics with the amalgamation of solar thermal, geothermal and hydro units

The elementary thermal system stated in segment 5.1 is at present state united with solar thermal in arena-1, geothermal in arena-2 and hydro unit in arena-3. The finest achieved controller PI(FOPD) from sector 5.1 along with HPA-ISE is employed here. Correspondingly, ARO is enforced to acquire its best grade of gains and related parameters. The ideal grades are specified in Table 5. And the equivalent observation is strategized in Figure 8. Widespread valuation of Figure 8, statuses that observation displays enhanced outcomes with much diminished Pk_O, Pk_U, S_Time when the scheme is unified with solar thermal, geothermal, and hydro elements.

Table 5: Outstanding gains and correlated parameters of PI(FOPD) subordinate controller via ARO for thermal system with integration of solar thermal, geothermal and hydro units

$K_{P1(PI(FOPD))} = 0.0012$	$K_{I1(PI(FOPD))} = 0.9796$	$K_{KP1(PI(FOPD))} = 0.0018$
$K_{KD1(PI(FOPD))} = 0.8578$	$\mu_{1(PI(FOPD))} = 0.0017$	$K_{P2(PI(FOPD))} = 0.0037$
$K_{I2(PI(FOPD))} = 0.9798$	$K_{KP2(PI(FOPD))} = 0.0017$	$K_{KD2(PI(FOPD))} = 0.9518$
$\mu_{2(PI(FOPD))} = 0.0018$	$K_{P3(PI(FOPD))} = 0.0028$	$K_{I3(PI(FOPD))} = 0.9785$
$K_{KP3(PI(FOPD))} = 0.0017$	$K_{KD3(PI(FOPD))} = 0.9448$	$\mu_{3(PI(FOPD))} = 0.0013$

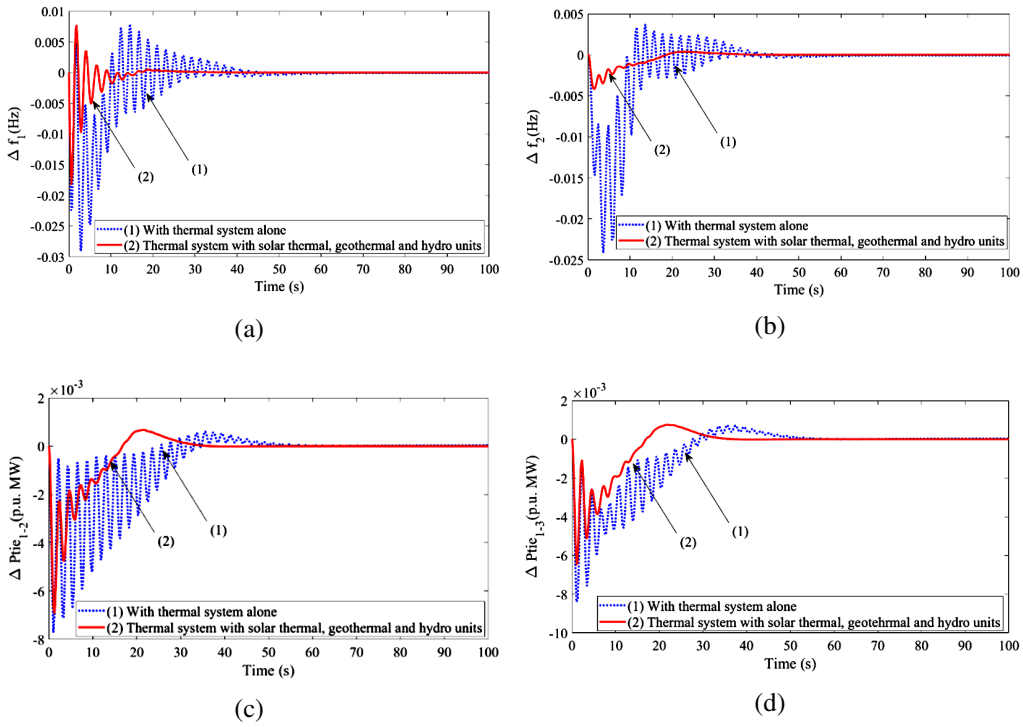

Figure 8: Diagram of deflection in dynamic observation for scheme with amalgamation of solar thermal, geothermal and hydro units contrast time:(a) Deflection of frequency observation of arena-1, (b) Deflection of frequency observation of arena-2, (c) Deflection in tie-line power interlinking arena-1 and arena-2, (d) Deflection in tie-line power interlinking arena-1 and arena-3

5.6. Valuation of scheme dynamics with incorporation of RFB

Here and now, scheme stated in sub-segregation 5.3 is combined with an energy storing device titled as RFB in all the arenas. This new-fangled scheme is also provided with PI(FOPD) controller, HPA-ISE and ARO is utilised to acquire its outstanding standards of gains in addition related constraints. The outstanding expected values are recorded in Table 6 in addition conforming potent observation are replicated in Figure 9a–9d. Widespread inspection of Figure.9 articulates around the healthier presentation of observation through amalgamation of RFB regarding lessened Pk_O, Pk_U and S_Time.

Table 6: Outstanding Gains and correlated parameters of PI(FOPD) subordinate controller for scheme with RFB using ARO

$K_{P1(PI(FOPD))} = 0.1342$	$K_{I1(PI(FOPD))} = 0.9946$	$K_{KP1(PI(FOPD))} = 0.2178$
$K_{KD1(PI(FOPD))} = 0.9489$	$\mu_{1(PI(FOPD))} = 0.0187$	$K_{P2(PI(FOPD))} = 0.3411$
$K_{I2(PI(FOPD))} = 0.8516$	$K_{KP2(PI(FOPD))} = 0.1778$	$K_{KD2(PI(FOPD))} = 0.9519$
$\mu_{2(PI(FOPD))} = 0.0197$	$K_{P3(PI(FOPD))} = 0.3031$	$K_{I3(PI(FOPD))} = 0.8586$
$K_{KP3(PI(FOPD))} = 0.1899$	$K_{KD3(PI(FOPD))} = 0.7529$	$\mu_{3(PI(FOPD))} = 0.0154$

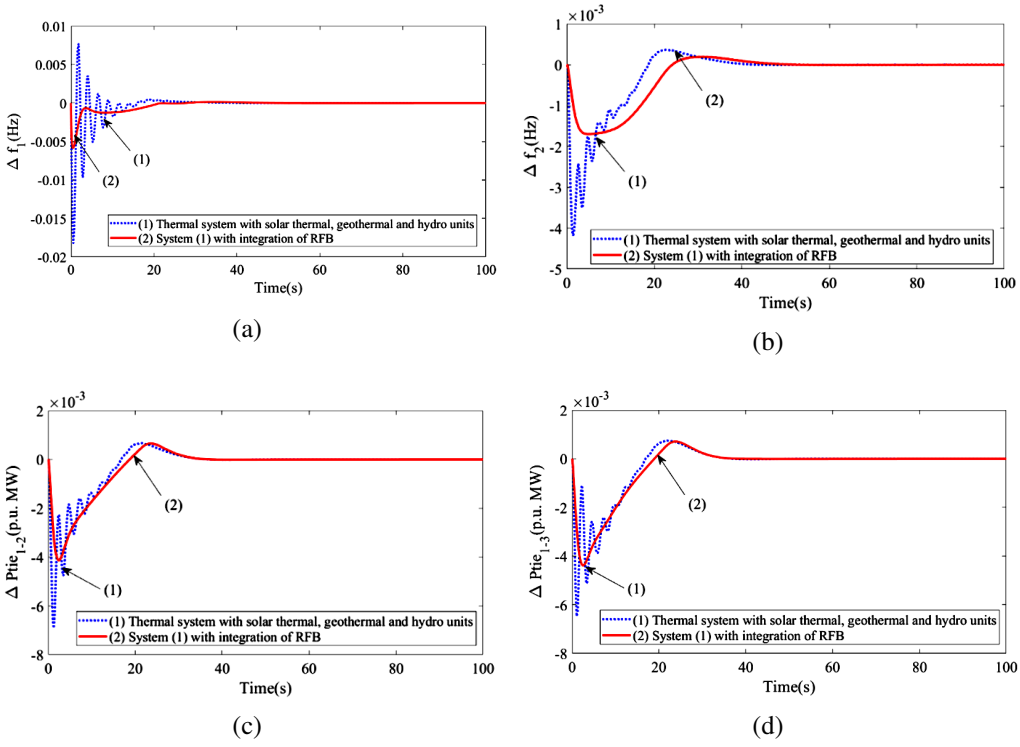

Figure 9: Design of deflection in dynamic observation for scheme with amalgamation of RFB contrast time: (a) Deflection of frequency observation of arena-1, (b) Deflection of frequency observation of arena-2, (c) Deflection in tie-line power interlinking arena-1–arena-2, (d) Deflection in tie-line power interlinking arena-1–arena-3

5.7. Sensitivity valuation to inspect heftiness of proposed PI(FOPD) with ARO

Now in the current sub-category, dynamic observation of the scheme with RFB are evaluated for higher order SLP of 3% from basic 1% SLP. The dynamic observation is plotted using PI(FOPD) controller and its gains and parameters

are collected by HPA-ISE with the usage of ARO. The finest values of PI(FOPD) controller with ARO at 3% SLP is enlisted in Table 7 and the conforming dynamic observation are evaluated in Figure 10a–10d. Valuation of Figure 10 articulates that the observations attained are nearly analogous and requires no added alterations.

Table 7: Gains and other related parameters of PI(FOPD) controller with ARO for 3% SLP

$K_{P1(PI(FOPD))} = 0.2215$	$K_{I1(PI(FOPD))} = 0.9867$	$K_{KP1(PI(FOPD))} = 0.4257$
$K_{KD1(PI(FOPD))} = 0.7956$	$\mu_{1(PI(FOPD))} = 0.0145$	$K_{P2(PI(FOPD))} = 0.5141$
$K_{I2(PI(FOPD))} = 0.7811$	$K_{KP2(PI(FOPD))} = 0.1987$	$K_{KD2(PI(FOPD))} = 0.5943$
$\mu_{2(PI(FOPD))} = 0.0176$	$K_{P3(PI(FOPD))} = 0.3124$	$K_{I3(PI(FOPD))} = 0.6865$
$K_{KP3(PI(FOPD))} = 0.2134$	$K_{KD3(PI(FOPD))} = 0.7867$	$\mu_{3(PI(FOPD))} = 0.0187$

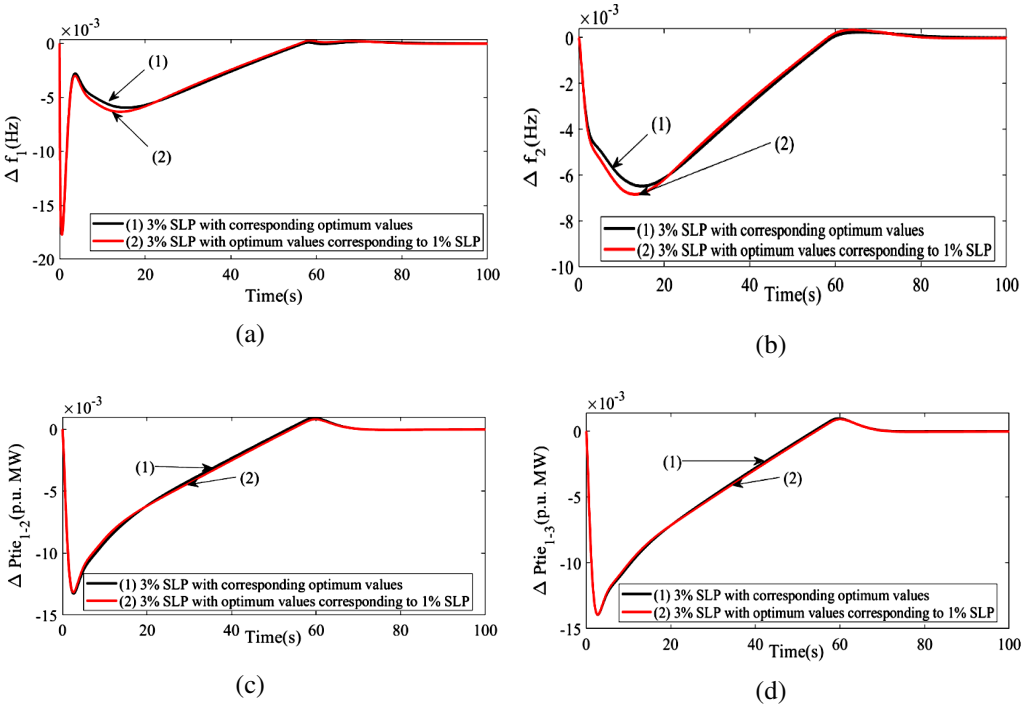

Figure 10: Diagram of deflection in dynamic observation for scheme with SLP of 3% contrast time: (a) Deflection of frequency observation of arena-1, (b) Deflection of frequency observation of arena-2, (c) Deflection in tie-line power interlinking arena-1–arena-2, (d) Deflection in tie-line power interlinking arena-1–arena-3

6. Conclusion

In the current piece of work, an innovative optimization action named by ARO inclusive of PI(FOPD) controller is proficiently employed in the examined triple-area structure of scheme. A maiden effort was made to utilize HPA-ISE as a performance index and studies shows that HPA-ISE outperforms over ISE. The scheme's dynamic observation are evaluated contemplating PI, PID and PI(FOPD) controllers. Additionally, PI(FOPD) controller yield spectacular execution in association with peak value anomaly and duration of settling associated to added controllers. The examination is taken frontward for contrast of ARO with added optimization practices alike FA then GWO. Examination evidently demonstrates the improved conduct of ARO as it converges quicker with modest values. Also, studies are carried with various ACR and investigations reveal that with high value of ACR, the system dynamics are enhanced. Moreover, amalgamation of solar thermal in arena-1, geothermal in arena-2 and hydro units in arena-3 with thermal systems displays improved outcomes over thermal. Added integration of RFB in all areas advances dynamics of the scheme. Sensitivity analysis with higher value of SLP suggests that proposed PI(FOPD) controller is robust and demands no further amendments.

ADDENDUM

Nominal scheme Parameters: $F = 60$ Hz, $T_{jk,AC} = 0.086$pu MW/rad, $H_j = 5$ s, $K_{pj} = 120$ Hz/MW pu, $D_j = 8.33 \cdot 10^{-3}$ pu MW/Hz, $B_j = 0.425$ pu MW/Hz, $R_j = 2.4$ pu MW/Hz, $T_{gj} = 0.08$ s, $T_{tj} = 0.3$ s, $T_{rj} = 10$ s, $K_{rj} = 0.5$ s, $T_{pj} = 20$ s, $Ks_j = 1.8$, $Ts_j = 1.8$ s, SLP = 1%, loading = 50%, $P_{r1} = 1000$ MW, $P_{r2} = 2000$ MW, $K_{\mathrm{DC}} = 0.5$, $T_{\mathrm{DC}} = 0.03$ s. Hydro: $K_d = 4$, $K_p = 1$, $K_i = 5$, $T_w = 1$ s; Solar scheme: $T_{ss} = 1.8$ s, $K_{ss} = 1.8$, $T_{tss} = 3.0$ s, $T_{gss} = 1.0$ s; RFB: $K_r = 1$, $T_d = 0$, $T_r = 0.78$ s, $K_{\mathrm{RFB}} = 1.8$.

References

[1] O.I. Elgerd: *Electric energy systems theory: an introduction*. Tata McGraw-Hill, New Delhi, 2007.

[2] P. Kundur: *Power system stability and control*. Tata McGraw Hill, New Delhi, 5th edition, 1993.

[3] H. Golpira, H. Bevrani and H. Golpira: Application of GA optimization for automatic generation control design in an interconnected power system. *Energy Conversion and Management*. **52**(5) (2011), 2247–2255. DOI: 10.1016/j.enconman.2011.01.010.

[4] J. Nanda, A. Mangla andd S. Suri: Some new findings on automatic generation control of an interconnected hydrothermal system with conventional controllers. *IEEE Transactions on Energy Conversion*, **21**(1), (2006), 187–194. DOI: 10.1109/TEC.2005.853757.

[5] Y. Sharma and L.C. Saikia: Automatic generation control of a multi-area ST–thermal power system using Grey Wolf optimizer algorithm based classical controllers. *International Journal of Electrical Power and Energy Systems*, **73** (2015), 853–862. DOI: 10.1016/j.ijepes.2015.06.005.

[6] A. Saha and L.C. Saikia: Utilization of ultra-capacitor in load frequency control under restructured STPP-thermal power systems using WOA optimized PIDN-FOPD controller. *IET Generation, Transmission and Distribution*, **11**(13), (2017), 3318–3331. DOI: 10.1049/iet-gtd.2017.0083.

[7] W. Tasnin and L.C. Saikia: Maiden application of an sine–cosine algorithm optimised FO cascade controller in automatic generation control of multi-area thermal system incorporating dish-Stirling solar and geothermal power plants. *IET Renewable Power Generation*, **12**(5), (2018), 585–597. DOI: 10.1049/iet-rpg.2017.0063.

[8] A. Saha and L.C. Saikia: Load frequency control of a wind-thermal-split shaft gas turbine-based restructured power system integrating FACTS and energy storage devices. *International Transactions on Electrical Energy Systems*, **29**(3), (2018). DOI: 10.1002/etep.2756.

[9] I. Pan and S. Das: Fractional order AGC for distributed energy resources using robust optimization. *IEEE Trans on Smart Grid*, **7**(5), (2016), 2175–2186. DOI: 10.1109/TSG.2015.2459766.

[10] J. Nanda, S. Mishra and L.C. Saikia: Maiden application of bacterial foraging-based optimization technique in multiarea automatic generation control. *IEEE Transactions on Power Systems*, **24**(2), (2009), 602–609. DOI: 10.1109/TPWRS.2009.2016588.

[11] O. Singh and I. Nasiruddin: Optimal AGC regulator for multi-area interconnected power systems with parallel AC/DC links. *Cogent Engineering Journal*, **3**(1), (2018). DOI: 10.1080/23311916.2016.1209272.

[12] K. Jagatheesan, B. Anand, S. Samanta, N. Dey, A.S. Ashour and V.E. Balas: Design of a proportional-integral-derivative controller for an automatic generation control of multi-area power thermal systems using firefly algorithm. *IEEE/CAA Journal of Automatica Sinica*, **6**(2), (2019), 503–515. DOI: 10.1109/JAS.2017.7510436.

[13] M. Raju, L.C. Saikia, N. Sinha and D. Saha: Application of antlion optimizer technique in restructured automatic generation control of two-area

hydro-thermal system considering governor dead band. Proceedings of the Conference on *Innovations in Power and Advanced Computing Technologies*, Vellore, India, (2017). DOI: 10.1109/IPACT.2017.8245099.

[14] L.C. Saikia, A. Chowdhury, N. Shakya, S. Shukla and P.K. Soni: AGC of a multi area gas-thermal system using firefly optimized IDF controller. *Annual IEEE India Conference (INDICON)*, (2013), India.

[15] A. Rahman, L.C. Saikia and N. Sinha: Load frequency control of a hydro-thermal system under deregulated environment using biogeography-based optimised three-degree-of freedom integralderivative controller. *IET Generation, Transmission and Distribution*, **9**(15), (2015), 2284–2293. DOI: 10.1049/iet-gtd.2015.0317.

[16] G. Sharma, K.R. Ibraheem Niazi and R.C. Bansal: Adaptive fuzzy critic based control design for AGC of power system connected via AC/DC tie-lines. *IET Generation, Transmission and Distribution*, **11**(2), (2016), 560–569. DOI: 10.1049/iet-gtd.2016.1164.

[17] P. Dash, L.C. Saikia and N. Sinha: Flower pollination algorithm optimized PI-PD cascade controller in automatic generation control of a multi-area power system. *International Journal of Electrical Power and Energy Systems*, **82** (2016), 19–28. DOI: 10.1016/j.ijepes.2016.02.028.

[18] X.S. Yang: *Nature-Inspired Meta-Heuristic Algorithms*. Beckington, UK, Luniver Press, 2008.

[19] N.R. Babu, S.K. Bhagat, L.C. Saikia, T. Chiranjeevi, R. Devarapalli and F.P. García Márquez: A comprehensive review of recent strategies on automatic generation control/load frequency control in power systems. *Archives of Computational Methods in Engineering*, **30**(1), (2022). DOI: 10.1007/s11831-022-09810-y.

[20] B. Venkateswara Rao, R. Devarapalli, H. Malik, S.K. Bali, F.P. García Márquez and T. Chiranjeevi: Wind integrated power system to reduce emission: An application of Bat algorithm. *Journal of Intelligent and Fuzzy Systems*, **42**(2), (2022), 1041–1049. DOI: 10.3233/JIFS-189770.

[21] A. Saha, P. Dash, N.R. Babu, T. Chiranjeevi, B. Venkateswararao and Ł. Knypiński: Impact of spotted hyena optimized cascade controller in load frequency control of wave-solar-double compensated capacitive energy storage based interconnected power system. *Energies*, **15**(19), (2022). DOI: 10.3390/en15196959.

[22] X.S. Yang: Firefly algorithms for multimodal optimization. In: *Stochastic Algorithms: Foundations and Applications*, SAGA 2009, Lecture Notes in

Computer Sciences, **5792**, (2009), 169–178. DOI: 10.48550/arXiv.1003.1466.

[23] S. Mirjalili, S.M. Mirjalili and A. Lewis: Grey Wolf optimizer. *Advances Engineering Software*, **69** (2014), 46–61. DOI: 10.1016/j.advengsoft.2013.12.007.

[24] L. Wang, Q. Cao, Z. Zhang, S. Mirjalili and W. Zhao: Artificial rabbits optimization: A new bio-inspired meta-heuristic algorithm for solving engineering optimization problems. *Engineering Applications of Artificial Intelligence*, **114** (2022), DOI: 10.1016/j.engappai.2022.105082.

[25] N. Pathak and Z. Hu: Hybrid-peak-area-based performance index criteria for AGC of multi-area power systems. *IEEE Transactions on Industrial Informatics*, **15**(11), (2019), 5792–5802. DOI: 10.1109/TII.2019.2905851.

[26] N.R. Babu and L.C. Saikia: Optimal location of accurate HVDC and energy storage devices in a deregulated AGC integrated with PWTS considering HPA-ISE as performance index. *Engineering Science and Technology, an International Journal*, **33** (2022). DOI: 10.1016/j.jestch.2021.10.004.

[27] T. Chiranjeevi and R.K. Biswas: Discrete-time fractional optimal control. *Mathematics*, **5**(2), (2017), 1–12. DOI: 10.3390/math5020025.

[28] T. Chiranjeevi and R.K. Biswas: Closed-form solution of optimal control problem of a fractional order system. *Journal of King Saud University – Science*, **31**(4), (2019), 1042–1047. DOI: 10.1016/j.jksus.2019.02.010.

[29] T. Chiranjeevi, R.K. Biswas, R. Devarapalli, N.R. Babu and F.P. García Márquez: On optimal control problem subject to fractional order discrete time singular systems. *Archives of Control Sciences*, **31**(4), (2021), 849–863. DOI: 10.24425/acs.2021.139733.

[30] T. Chiranjeevi, R. Devarapalli, N.R. Babu, K.B. Vakkapatla, R. Gowri Sankara Rao and F.P. García Márquez: Fixed terminal time fractional optimal control problem for discrete time singular system. *Archives of Control Sciences*, **32**(3), (2022), 489–506. DOI: 10.24425/acs.2022.142846.

[31] A. Oustaloup, B. Mathieu, and P. Lanusse: The CRONE control of resonant plants: Application to a flexible transmission. *European Journal of Control*, **1**(2), (1995), 113–121. DOI: 10.1016/S0947-3580(95)70014-0.